Simulation of flow in a continuous galvanizing bath: Part II. Transient aluminum distribution resulting from ingot addition

Ajersch, F.; Ilinca, F.; Hétu, J.-F.

Publisher's version / Version de l'éditeur:
https://doi.org/10.1007/s11663-004-0107-4
Metallurgical and Materials Transactions B, 35B, 1, pp. 171-178, 2004-02-01

Simulation of Flow in a Continuous Galvanizing Bath: Part II. Transient Aluminum Distribution Resulting from Ingot Addition

F. AJERSCH, F. ILINCA, and J.-F. HÉTU

The coupled phenomena of momentum, heat, and mass transfer were simulated in order to predict and to better understand the generation and movement of intermetallic dross particles within certain regions of a typical galvanizing bath. Solutions for the temperature and aluminum concentration can be correlated with the solubility limits of aluminum (Al) and iron (Fe) to determine the amount of precipitated aluminum in the form of Fe_2Al_5 top dross. Software developed by the Industrial Materials Institute of the National Research Council of Canada (IMI-NRC), including k-ε turbulence modeling for heat and mass transfer, was adapted for the simulation of a sequence of operating parameters. Each case was modeled over a period of 1 hour, taking into account an ingot-melting period followed by a nonmelting period. The presence of an ingot significantly changes the temperature distribution and also results in important variations in the local aluminum concentration, since the makeup ingot has a higher aluminum concentration. The simulation showed that during the ingot melting, the total aluminum concentration is higher at the ingot side of the bath than at the strip exit side. The region below the ingot presents the highest aluminum concentration, whereas lower aluminum concentrations were found in the region above the sink roll, between the strip and the free surface. It was shown that precipitates form near the ingot surface because this region is surrounded by a solution at 420 °C, which is lower than the average bath temperature of 460 °C. When no ingot is present, the total aluminum concentration becomes much more uniform and decreases with time at a constant rate, depending on the coating thickness. This information is of major significance in the prediction of the formation of dross particles, which can cause defects on the coated product.

I. INTRODUCTION

AS a companion to the first part of this article,[1] this subsequent study takes into account the variation of the solubility of the aluminum and iron in a galvanizing bath as a result of local temperature variations. The previous article showed that the temperature variations are caused by the periodic additions of the cold zinc ingots, which take a finite time to melt, followed by a period when no additions are made to the bath. During ingot melting, the induction heaters operate at maximum capacity and heat input is reduced to a level of 20 pct of this value after melting, maintaining an average bath temperature of 460 °C.

The previous article simulated the flow and temperature distribution at steady-state conditions for the case of no ingot present and for the melting-ingot case. Since the surface of the melting ingot is at 420 °C, this condition represents the most severe temperature variation in the bath, since the energy to melt the ingot needs to be supplied by induction heaters. Tests have been carried out in industry by Toussaint *et al.*[2] to experimentally determine the duration of the melting period of a 1-ton ingot. They also modeled the melting period numerically, showing that the total time for melting is very close to 20 minutes for complete immersion. This period includes a 6-minute period during which the cold ingot freezes a layer of zinc from the bath onto the surface, followed by a period when the ingot heats up to the melting temperature and starts to melt back. As a result, the ingot actually starts to melt only after this 6-minute period. The melting rate decreases as the ingot is consumed. All the aluminum contained in the melting ingot is transferred to the bath and can be in precipitated form as Fe_2Al_5 or in solution, depending on the temperature of the bath. Particles precipitated in the coldest region of the bath can be displaced by the bath flow and can dissolve or grow in different regions, according to the solubility limits defined by thermodynamic relationships[3] and by growth kinetics.

In view of the transient period of ingot immersion, melting, and no ingot addition, it becomes essential to model the entire cycle of operation of a normal coating operation. The simulations use industrial data for the melting rate and coating rate to account for the mass balance of the process. A period of 1 hour was chosen, where the average total aluminum content of the bath and the temperature return to values close to the initial conditions at the start of the cycle, so that the simulations could show the dissolution and transport of the aluminum from the ingot to the coated steel strip. The objective of this article is to compute the spatial and temporal distribution of the aluminum content within the bath during a normal galvanizing operation. In order to carry out this task, data on the solubility limits of aluminum with temperature need to be integrated into the solution in order to distinguish between the amount of dissolved and precipitated aluminum (as Fe_2Al_5) in a typical operation.

F. AJERSCH, Professor, is with École Polytechnique de Montréal, Montréal, PQ, Canada H3C 3A7. F. ILINCA and J.-F. HÉTU, Research Officers, are with the Industrial Materials Institute, National Research Council, Boucherville, PQ, Canada J4B 6Y4. Contact e-mail: florin.ilinca@cnrc-nrc.gc.ca

Manuscript submitted April 3, 2003.

II. METHODOLOGY

The dimensions and configuration of the immersed equipment of the galvanizing bath are presented in Figure 1 of Part I of this article, and the computational domain was identical to that used previously. The strip width is 1500 mm, moving at 1.75 m/s and entering the bath at 460 °C. The simulation is carried out in the following steps for a total cycle of 60 minutes.

1. Solving for an initial solution (step 1):
   a. Solution 1.1 is obtained for the steady-state case without an ingot and without temperature-induced buoyancy effects.
   b. Solution 1.2 is obtained for the case without an ingot, but with temperature-induced buoyancy effects in the transient regime for a period of 20 minutes and using solution 1.1 as the initial condition. This solution takes into account the effect of the inductor heating input at low power.
2. Solving configuration A (with an ingot), in the transient regime, for a period of 20 minutes using solution 1.2 as the initial solution.
3. Solving configuration B (without an ingot), in the transient regime, for a period of 40 minutes after the 20-minute ingot-melting period, using the solution with an ingot (configuration A) as the initial condition.

III. PHYSICAL MODEL AND GOVERNING EQUATIONS

The Navier–Stokes equations for nonisothermal flow were solved, taking into account the variation in density due to the temperature and aluminum concentration using the Boussinesq approximation. Hence, the gravity term is considered as the perturbation from a reference value, and the momentum equations become

$$\rho_0 \frac{D\mathbf{u}}{Dt} = -\nabla p + \nabla \cdot \left(2(\mu + \mu_T)\dot{\gamma}(\mathbf{u})\right) - \rho_0 \mathbf{g}\beta_T (T - T_0) - \rho_0 \mathbf{g}\beta_{\mathrm{Al}}(c - c_0) \quad [1]$$

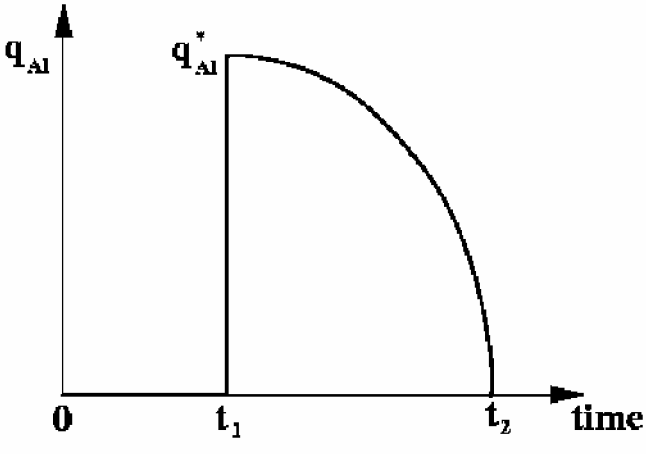

Fig. 1—Time evolution of the aluminum mass flux on the ingot surface.

where T is the temperature, c is the aluminum concentration, and ρ_0 is the density at the reference temperature T_0 and reference aluminum concentration c_0, while β_T and β_{Al} are the thermal- and aluminum-concentration expansion coefficients, defined as

$$\beta_T = -\frac{1}{\rho}\left(\frac{\partial \rho}{\partial T}\right)_{p,\,c} \quad [2]$$

$$\beta_{\mathrm{Al}} = -\frac{1}{\rho}\left(\frac{\partial \rho}{\partial c}\right)_{p,\,T} \quad [3]$$

The turbulent viscosity (μ_T) is computed using the standard k-ε model of turbulence, as shown in Part I of this article. The temperature (T) is obtained by solving the energy equation. The aluminum concentration (c) is obtained by solving the mass-transport equation:

$$\rho \frac{Dc}{Dt} = \nabla \cdot \left((D + D_T)\nabla_c\right) \quad [4]$$

where D is the molecular diffusion coefficient. For this work, we consider that the Schmidt number $\mathrm{Sc} = \mu/D$ is equal to unity. The turbulent diffusion (D_T) is computed from

$$D_T = \frac{\mu_T}{\mathrm{Sc}_T} \quad [5]$$

where Sc_T is the turbulent Schmidt number, considered to be equal to unity.

Boundary Conditions

The boundary conditions for the flow and heat transfer were presented in Part I of this work. For the transient condition at maximum power, the inductor inlet velocity was fixed at 0.75 m/s with a temperature increase of 20 °C. Without an ingot present, the inductors run at 20 pct of maximum power, corresponding to an inlet velocity of 0.4 m/s and a temperature increase of 8 °C. The heat fluxes were calculated as in the previous article.

For the case of aluminum transport in the bath, the boundary and initial conditions must also be imposed for the aluminum concentration. The initial aluminum concentration in the bath is considered to be 0.14 pct in weight, and the bath is considered saturated in Fe at the initial temperature of 460 °C. The limit of solubility is given by[3]

$$\left(\frac{c_{\mathrm{Fe}}}{100}\right)^2 \left(\frac{c_{\mathrm{Al}}}{100}\right)^5 = \exp\left(0.064 - \frac{36133}{T + 273}\right) \quad [6]$$

where C_{Fe} and C_{Al} are the weight concentrations of Fe and Al expressed in a percentage (quantity in kilograms of Al or Fe for 100 kg of solution), and T is the temperature in degrees Celsius.

On the bath walls, we impose a zero normal mass flux for the aluminum concentration (no generation and consumption). The boundary conditions take into account the additional aluminum from the ingot and the aluminum consumption on the steel strip. Since ingots are added to the bath at ambient temperature, no aluminum is transferred to the bath until the ingot reaches the melting point. This was

found to take 6 minutes.[2] The melting time is, therefore, 14 minutes, during which all the aluminum and zinc in the ingot is transferred in the bath. Hence, the effective ingot mass flux is

$$(q_{Al})_{ingot} = \begin{cases} 0 & , t < t_1 \\ q^*_{Al}\left(1 - \dfrac{(t - t_1)^2}{(t_2 - t_1)^2}\right) & , t_1 < t < t_2 \end{cases} \quad [7]$$

with $t_1 = 6$ min and $t_2 = 20$ min (Figure 1), and q^*_{Al} being the initial flux of Al at $t = 6$ min, which is 2.143 times the average Al flux calculated for a total melting time of 20 minutes.

Aluminum consumption on the strip surface is assumed to take place on the first 0.35 m of the strip from its entry in the bath (corresponding to 0.2 seconds at a strip velocity of 1.75 m/s). The overall aluminum concentration of the coating is considered to be 0.4 pct by weight for a coating weight of 60 g/m^2 (0.06 kg/m^2) per side. The mean aluminum consumption flux is given by

$$(q_{Al})_{strip} = -\frac{0.06 \text{ kg/m}^2}{0.35 \text{ m}} V_{strip}\, c_{Al} \quad [8]$$

The mass flux is $(q_{Al})_{strip} = -0.3 c_{Al}$ kg/(m^{2}s) for a strip velocity of 1.75 m/s, with $c_{Al} = 0.4$.

Since the aluminum solubility in the bath varies with temperature as given by Eq. [6], any excess aluminum will be present in the form of precipitates of Fe_2Al_5 (top dross). Both dissolved aluminum and precipitated aluminum were calculated.

Physical properties of the melted zinc solution (zinc + 0.14 pct Al) are given subsequently:

a. density of $\rho = 6600$ kg/m^3;
b. laminar viscosity of $\mu = 0.004$ Pa·s;
c. specific heat of $c_p = 512$ J/kg·K;
d. thermal conductivity of $\lambda = 60$ W/m·K;
e. thermal-expansion coefficient of $\beta_T = 1.666 \cdot 10^{-4} K^{-1}$;
f. aluminum-concentration expansion coefficient of $\beta_{Al} = 1.444 \cdot 10^{-2}$.

IV. NUMERICAL RESULTS

Figure 2 shows the distribution of temperature on the symmetry plane. With an ingot present, the cold zinc melting from the ingot flows to the bottom of the bath, and the solution presents higher temperature gradients than for the case without an ingot. Figure 3 illustrates the distribution of total aluminum concentration on the symmetry plane for cases with and without an ingot. With an ingot present, we observe a higher level of aluminum near the ingot and a lower level of aluminum near the strip where aluminum consumption takes place. Without an ingot, the aluminum concentration becomes very uniform except for a region above the sink roll, where the aluminum concentration is smaller. This is indicative of a zone that does not readily mix with the zone in contact with the external side of the strip. In industrial practice, however, very little difference is observed in the total aluminum content of the coatings on either side of the strip. Even through the calculations show that the inner contact side is exposed to a lower aluminum content than the outer side, the reactivity of aluminum in solution with the iron substrate is very high in forming the inhibition layer, which contains the bulk of the aluminum content of the coating. The small differences of aluminum content in the regions of the bath in contact with the inner and outer surface of the strip do not seem to affect the total amount of aluminum in the overall coating.

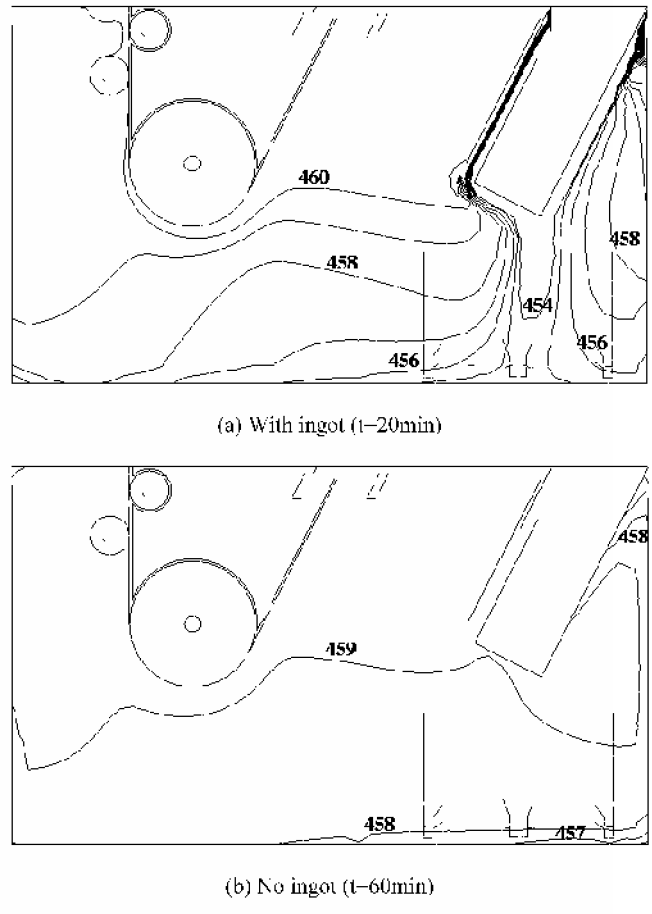

Fig. 2—Temperature distribution on the symmetry plane: (*a*) with ingot (t = 20 min) and (*b*) no ingot (t = 60 min) (increment between iso-values is 1 °C).

In order to illustrate the evolution of the aluminum distribution during an entire cycle of 20 minutes with an ingot and 40 minutes without an ingot, aluminum concentrations were calculated for four specific locations in the bath on the ingot side and also for four locations on the strip exit side. These locations are illustrated in Figure 4, with coordinates given in Table I. Figure 5 illustrates the evolution of the total aluminum concentration over the full cycle. This total aluminum represents the amount that is in solution as well as the amount that is in precipitated form. Subsequent calculations to differentiate between the dissolved and precipitated form of aluminum assume that the rates of dissolution and precipitation are instantaneous. The initial aluminum concentration is 0.14 ($t = 0$). During the first 6 minutes, the ingot is brought up to the melting point. During this period the aluminum concentration decreases, especially near the strip, as

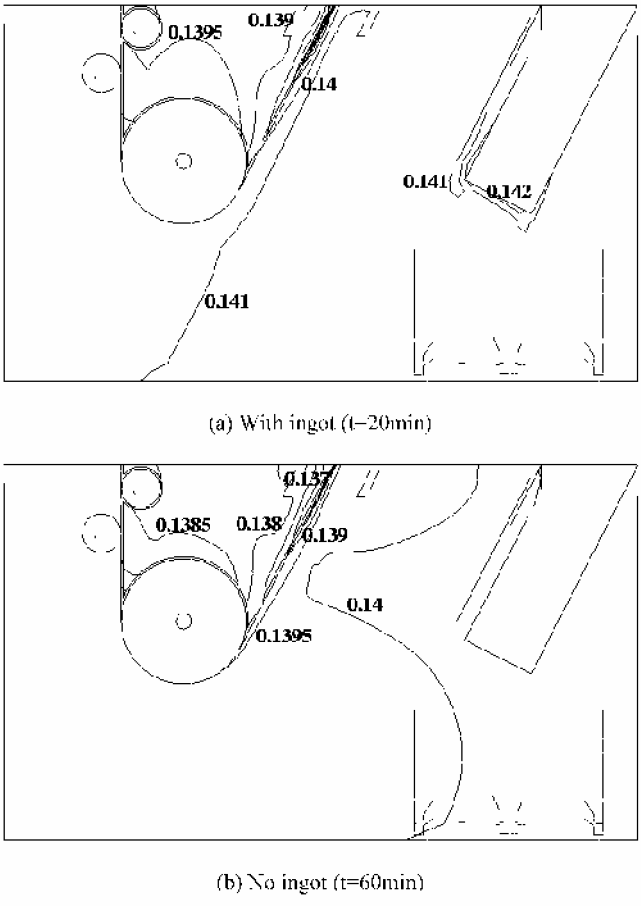

Fig. 3—Total aluminum concentration distribution on the symmetry plane: (*a*) with ingot (t = 20 min) and (*b*) no ingot (t = 60 min) (increment between iso-values is 0.0005).

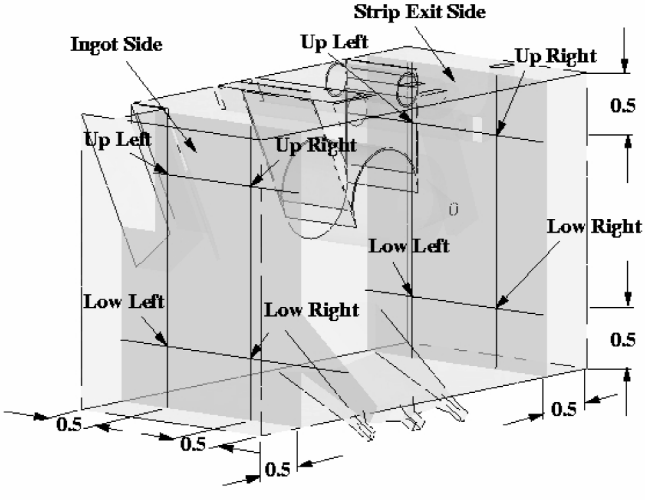

Fig. 4—Location of points for plots in time (dimensions are in meters).

aluminum consumption takes place on the strip without any supply from the ingot. When the ingot begins to melt (t = 6 min), a sharp increase of aluminum concentration is observed on the ingot side. On the strip exit side, the increase is delayed by about 3 minutes, corresponding to the time it takes for the zinc on the ingot side to reach the

Table I. Location of Points for Plots in Time

Location	Name	X (m)	Y (m)	Z (m)
Ingot side	up left	−1.55	−0.5	0.5
	up right	−1.55	−0.5	1.4
	low left	−1.55	−1.94	0.5
	low right	−1.55	−1.94	1.4
Strip exit side	up left	1.55	−0.5	0.5
	up right	1.55	−0.5	1.4
	low left	1.55	−1.94	0.5
	low right	1.55	−1.94	1.4

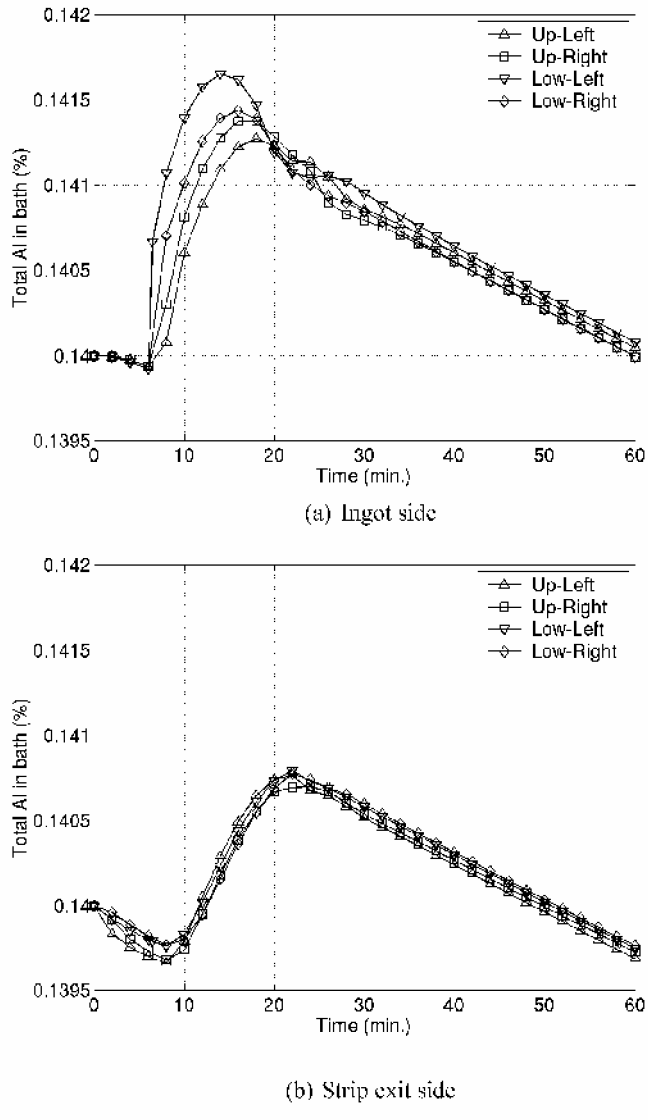

Fig. 5—Total aluminum concentration history on (*a*) the ingot side and (*b*) strip exit side.

front (strip section) of the bath as a result of the overall bath flow. Validation tests using aluminum sensors to measure the variations in aluminum level after the addition of brightener bars, presented in a previous study,[4] observed nearly the same value of the time increment, respectively, 3.6 minutes for the inductors operating at 100 pct and 2.4 minutes for the inductors operating at 50 pct. During ingot melting, the total aluminum concentration in the bath

is higher, with a maximum value near the ingot at about $t = 14$ min. On the ingot side, the differences between different locations are more apparent, resulting in larger values on the lower-left-hand-side location and the lowest values for the upper-left-hand-side location. Flow from the ingot (rich in aluminum) reaches the lower-left location first, followed by the lower-right, upper-right, and, finally, upper-left locations. This is also confirmed by the movement of zinc shown in the particle-trace figures.[1] On the strip exit side, the aluminum concentration is more uniform, since this area is mixed at a much higher intensity due to the roll and strip movement. Without an ingot, the aluminum concentration becomes more uniform but still remains higher on the ingot side. During this period, the aluminum concentration decreases constantly because of the aluminum consumption on the strip.

Figure 6 shows the temperature evolution at the same locations. It should be noted that the initial temperature is not uniform and corresponds to the distribution after 20 minutes for the configuration without an ingot, as was shown in Section II. As soon as the ingot is introduced into the bath ($t = 0$), the temperature drops at the inductor/ingot side at the lower-left and lower-right locations. The temperature rises at the upper-right location because inductors are running at higher power, projecting heated zinc toward the top surface of the bath. We can also observe that the temperature gradients are higher on the ingot side and during the ingot melting ($t = 0$ to 20 min). Without an ingot, the temperature remains almost constant after an initial correction between $t = 20$ and $t = 30$ minutes. The stratification of temperature in the bath is due to buoyancy and the calculated heat losses at the walls and surface. Figure 7 illustrates the concentration of aluminum precipitated as Fe_2Al_5 dross. This value is determined as the mass of aluminum above the temperature-dependent limit of solubility. When the ingot is immersed, we observe a sharp increase in dross formation on the ingot side. This is caused by the decrease in temperature, which is highest at the lower-left location. A second wave of dross formation is apparent during ingot melting, when the

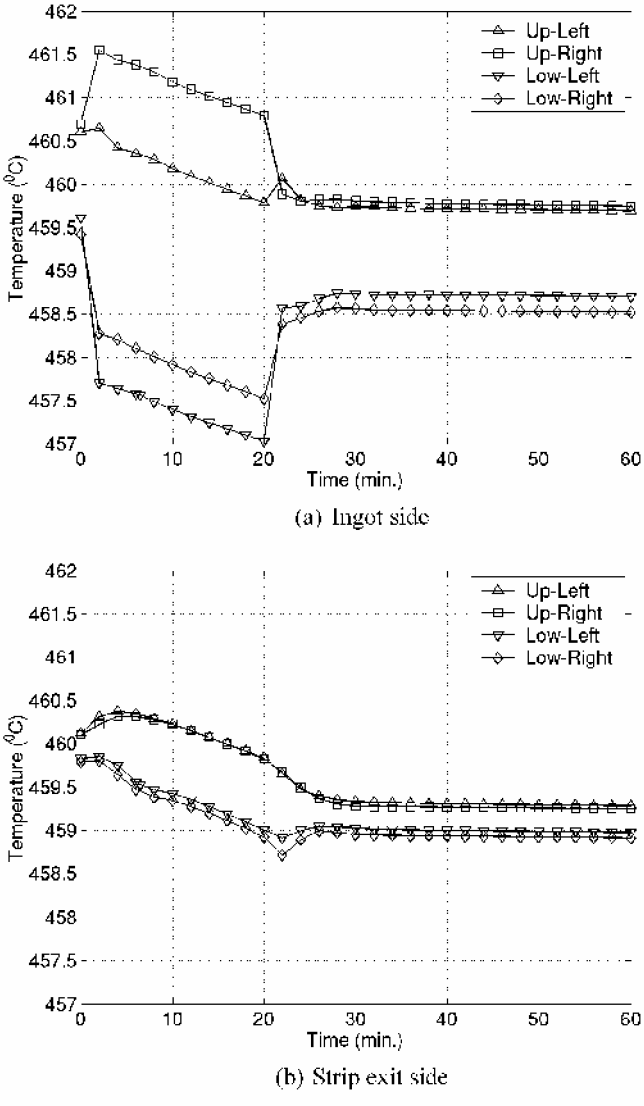

Fig. 6—Temperature history on (*a*) the ingot side and (*b*) strip exit side.

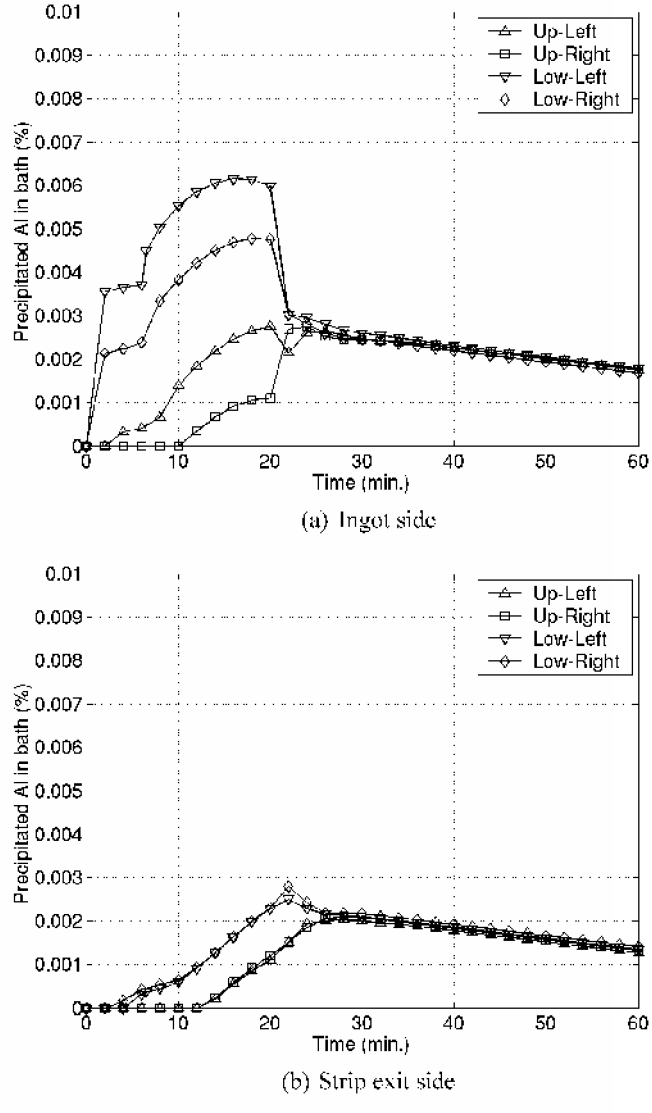

Fig. 7—History of the aluminum concentration as Fe_2Al_5 precipitate on (*a*) the ingot side and (*b*) strip exit side.

aluminum-rich ingot dissolves in the bath. Again, larger variations are observed on the ingot side. After 20 minutes, without an ingot present, the concentration of precipitate is rapidly stabilized and becomes more uniform. However, the values on the ingot side are slightly larger than on the strip exit side.

The solutions for two different values of aluminum concentration in the added ingot are compared. The solution for a 1 pct ingot is compared with the solution for a 0.5 pct ingot. Figure 8 illustrates the solution for the total aluminum concentration on the ingot side. Locations on the left-hand side are shown in Figure 8(a), while those on the right-hand side are shown in Figure 8(b), where the locations are defined as in Figure 4. As can be observed, the 1 pct ingot produces a higher total aluminum concentration. Since the total aluminum introduced to the bath is twice the value of the 0.5 pct ingot, during the same 20-minute period, the local concentration increase during the ingot-melting phase is about 2 times higher for the 1 pct ingot. During the period without an ingot, the aluminum concentrations in the bath decrease at nearly the same rate for both ingots. After melting, the 1 pct ingot contributes about 0.001 pct more aluminum to the bath than the 0.5 pct ingot. A similar observation can be made for the locations on the strip exit side shown in Figure 9. Differences are apparent only after 9 minutes, because the aluminum-concentration peak from the ingot side takes about 3 minutes to travel from the ingot to the strip exit side. The calculations show that for the 0.5 pct ingot, the final aluminum concentration returns back to a level near the initial value of 0.14 pct, while for the 1 pct ingot, the aluminum concentration at the end of the cycle is higher at about 0.141 pct. This solution confirms the practice of adding ingots of different aluminum contents to the bath, depending on the strip-width, strip-speed, and coating-weight requirements.

The comparison of the aluminum concentration as precipitated Fe_2Al_5 is shown in Figure 10 for the ingot side

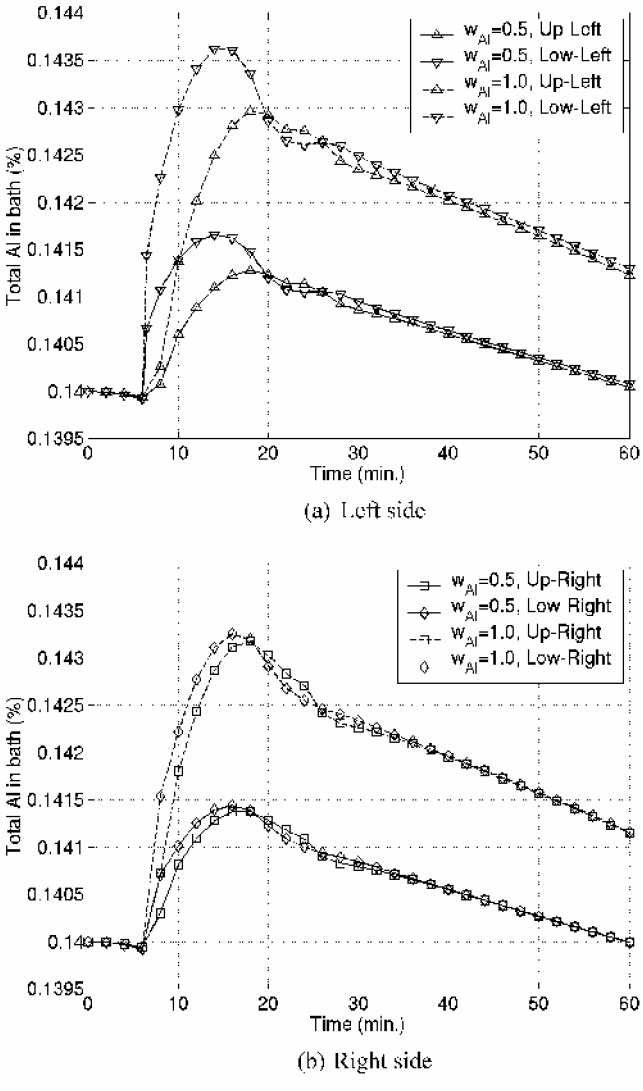

Fig. 8—(*a*) and (*b*) Effect of the aluminum concentration in ingot on the total aluminum concentration history in the bath on the ingot side.

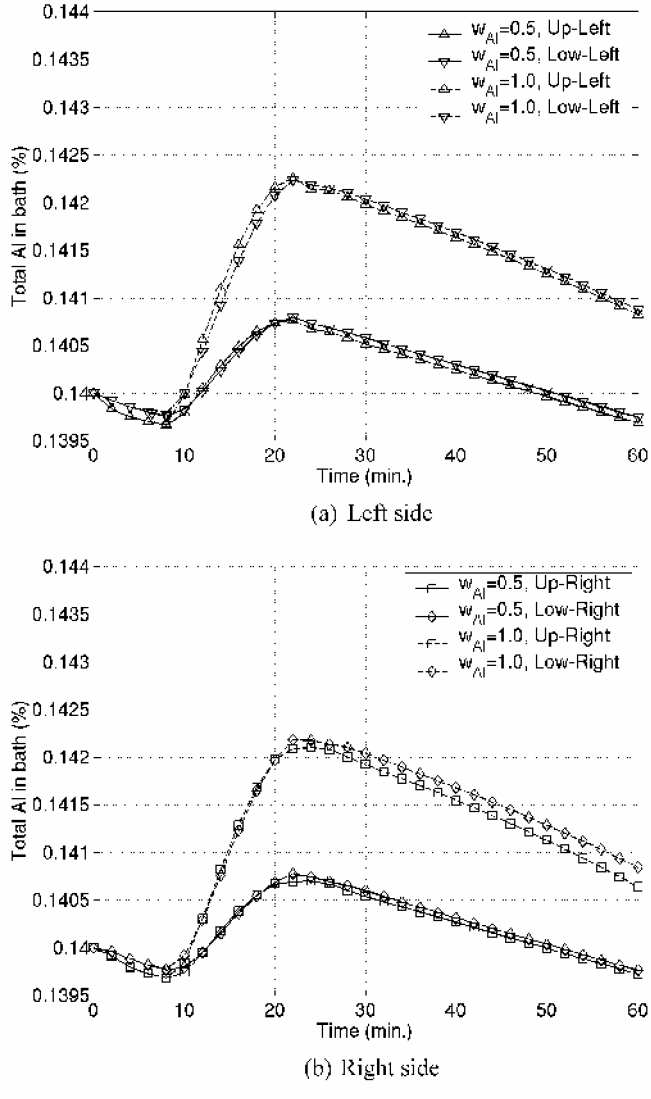

Fig. 9—(*a*) and (*b*) Effect of the aluminum concentration in ingot on the total aluminum concentration history in the bath on the strip exit side.

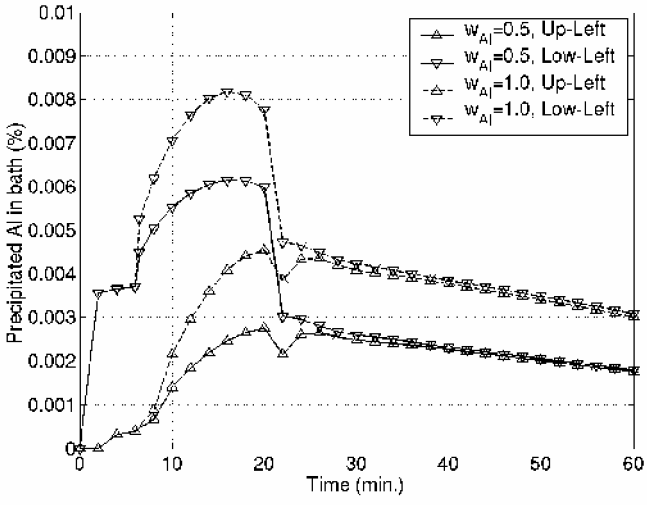

(a) Left side

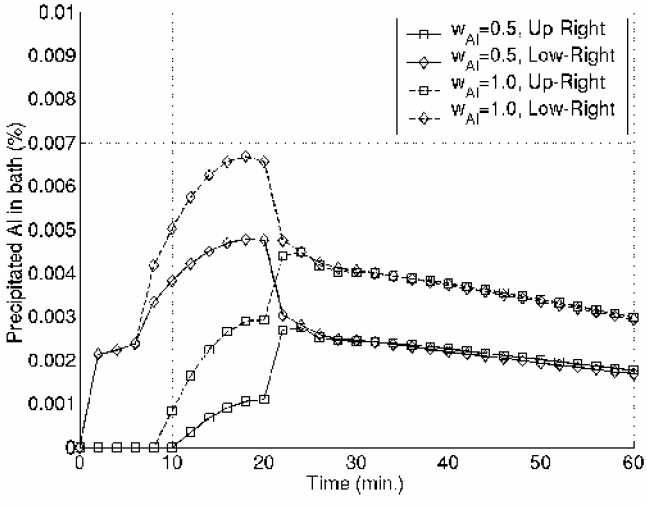

(b) Right side

Fig. 10—(*a*) and (*b*) Effect of the aluminum concentration in ingot on the aluminum concentration as Fe_2Al_5 precipitate in the bath on the ingot side.

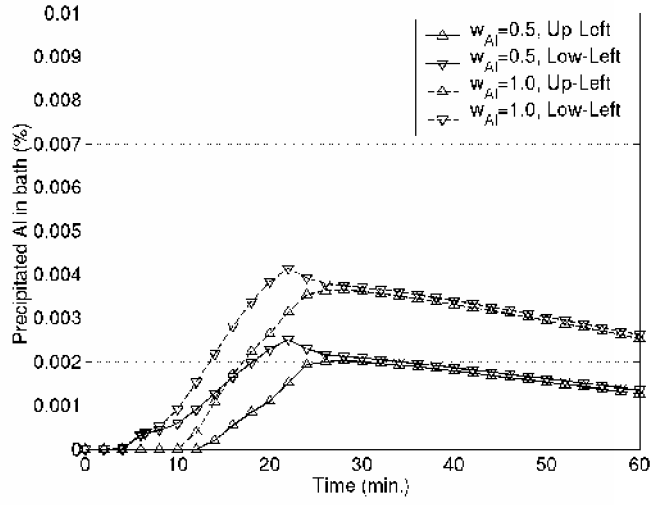

(a) Left side

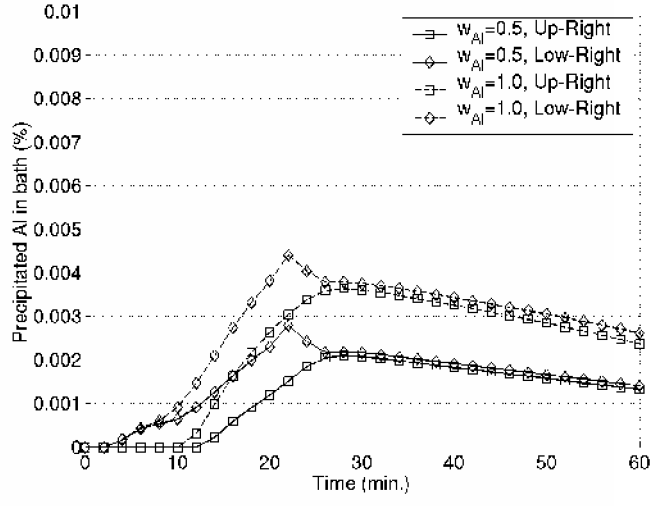

(b) Right side

Fig. 11—(*a*) and (*b*) Effect of the aluminum concentration in ingot on the aluminum concentration as Fe_2Al_5 precipitate in the bath on the strip exit side.

and in Figure 11 for the strip exit side. During the first 6 minutes, no aluminum is added by the ingot and, hence, solutions are identical. The increase in precipitated Al as Fe_2Al_5 is due to the decreased solubility resulting from the decreased temperature during the immersion and melting of the ingot. During ingot melting (the time from 6 to 20 minutes), a larger amount of dross is formed for all locations. As the ingot melts, the precipitated Al increases rapidly, reaching a maximum at around 20 minutes. The values decrease after the ingot is molten, and the temperature at these locations is re-established by inductor mixing to the control value of 460 °C for the average bath temperature, where the local temperatures return to the values shown in Figure 6. The effect of changing the aluminum concentration in the ingot is more evident at the inductor/ingot side. As previously observed, the quantity of aluminum precipitated at the end of the cycle is larger, by almost 0.001 pct, than for the case of the 0.5 pct ingot.

V. DISCUSSION

The coupled mass- and heat-transfer solutions have resulted in a clear and consistent representation of the distribution of aluminum in the bath for a simulated cycle of an ingot-melting period followed by a period with no ingot in the bath. As the ingot melts, the local total aluminum content increases according to the temperature- and motion-induced flows. Since the ingot melts during this initial period, the total aluminum represents the amount in solution and the amount that is in precipitated form. Assuming that the precipitated form of aluminum is Fe_2Al_5 and is very finely dispersed, it will be displaced at the same speed as the liquid zinc in the bath. When these particles are transported into the region of higher temperature, they are assumed to dissolve instantly according to the solubility limits.

The series of solutions for the aluminum distribution is consistent with the rate of dissolution of an ingot and the uptake of aluminum from the bath. For a normal operation

at a 1.75 m/s strip speed and a coating weight of 60 g/m^2, the value of the aluminum content rises during the ingot-melting stage and returns to about the same value after the total period of a 1-hour cycle. If 1 pct ingots are used instead of 0.5 pct ingots, the value of the total aluminum content at the end of the cycle is higher, as would be expected. This confirms the need to vary the ingot composition for different coated products, taking into account the strip width, strip speed, and coating weight.

Since the reaction kinetics of the formation of the inhibition layer are very fast and are essentially the same for the small variations of dissolved aluminum in the bath, the overall aluminum content of the coating on each side of the strip is almost the same. If the reaction kinetics were sensitive to these variations, the inside of the strip would have an overall lower aluminum content according to the solutions of aluminum distribution in the different regions of the bath.

In analyzing the series of solutions of the total and precipitated aluminum in the bath, calculated at the eight specific locations, we can observe that the amount of precipitated aluminum does not return to zero at the completion of the 60-minute cycle. Amounts from 0.001 to 0.006 pct Al remain in the bath beyond this period and will tend to circulate throughout the bath. This could explain the formation of larger particles of Fe_2Al_5 due to nucleation and growth of these particles over time, according to a mechanism described generally as Ostwald ripening.

VI. CONCLUSIONS

The numerical simulations carried out in this article show the spatial and temporal distribution of aluminum content in a typical galvanizing bath during a sequence of ingot addition and melting followed by a period when no ingot is present in the bath. Using the solubility limits of aluminum in the bath as a function of the bath temperature, it was clearly shown that the total and precipitated aluminum content can be monitored during this sequence. It can be concluded that the calculated aluminum-concentration gradients are much more pronounced at the inductor side during melting, whereas a more uniform distribution occurs during the period when no ingot is present. A more uniform distribution can be observed on the strip side compared to the ingot side, due to the high degree of mixing caused by the rotating equipment in this region. The aluminum concentration as precipitated Fe_2Al_5 also increases in the melting-ingot zone, primarily due to the decrease of temperature near the ingot surface and, also, because of the higher aluminum concentration of the ingot. The peak of the aluminum concentration shows a delay of about 3 minutes from the ingot side to the strip side. This delay is similar to the results obtained in the validation tests of the industrial bath. It is clearly shown that the heat input needs to be closely controlled during ingot melting to maintain a stable temperature of the bath. However, the inherent temperature gradients caused by ingot melting result in the precipitation of aluminum as Fe_2Al_5 in the cold regions of the bath.

ACKNOWLEDGMENTS

The authors acknowledge particularly Dr. F.E. Goodwin, the International Lead Zinc Research Organization (ILZRO), and the industrial sponsors for funding this project. The authors also acknowledge the contribution of Michel Perrault in creating the bath mesh for the simulation.

REFERENCES

1. F. Ajersch, F. Ilinca, and J.-F. Hétu: *Metall. Mater. Trans. B,* 2004, vol. 35B, pp. 161-70.
2. P. Toussaint, P. Vernin, L. Segers, R. Winand, and M. Dubois: *Ironmaking and Steelmaking,* 1995, vol. 22, pp. 171-76.
3. N.-Y. Tang: *J. Phase Equilibria,* 1996, vol. 17, pp. 396-98.
4. A. Paré, C. Binet, and F. Ajersch: *GALVATECH '95,* 1995, pp. 695-706.